Recombination dynamics and carrier lifetimes in highly mismatched ZnTeO alloys

Yan-Cheng Lin, Ming-Jui Tasi, Wu-Ching Chou, Wen-Hao Chang, Wei-Kuo Chen, Tooru Tanaka, Qixin Guo, and Mitsuhiro Nishio

---

Articles you may be interested in

Temperature-dependent decay dynamics in highly mismatched ZnSe1 x Te x alloy
Appl. Phys. Lett. **100**, 071912 (2012); 10.1063/1.3687187

Effect of CdS film thickness on the photoexcited carrier lifetime of TiO2/CdS core-shell nanowires
Appl. Phys. Lett. **99**, 153111 (2011); 10.1063/1.3651340

Effect of annealing on the structural and luminescent properties of ZnO nanorod arrays grown at low temperature
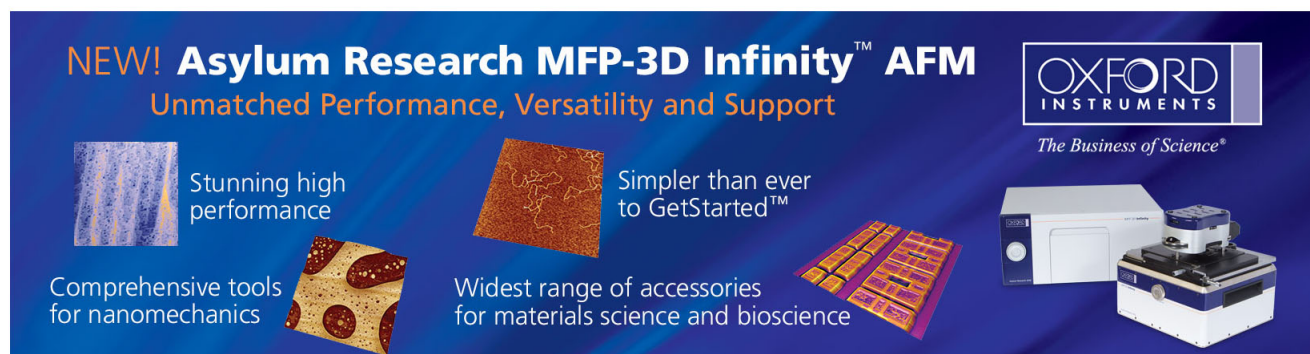J. Appl. Phys. **109**, 103508 (2011); 10.1063/1.3586243

Generation and recombination rates at ZnTe:O intermediate band states
Appl. Phys. Lett. **95**, 261107 (2009); 10.1063/1.3274131

Electrical control of spin coherence in ZnO
Appl. Phys. Lett. **92**, 162109 (2008); 10.1063/1.2913049

Recombination dynamics and carrier lifetimes in highly mismatched ZnTeO alloys

Yan-Cheng Lin,[1,a)] Ming-Jui Tasi,[1] Wu-Ching Chou,[1,a)] Wen-Hao Chang,[1] Wei-Kuo Chen,[1] Tooru Tanaka,[2,3] Qixin Guo,[4] and Mitsuhiro Nishio[2]

[1]*Department of Electrophysics, National Chiao Tung University, Hsinchu 30010, Taiwan*
[2]*Department of Electrical and Electronic Engineering, Saga University, Saga 840-8502, Japan*
[3]*PRESTO, Japan Science and Technology Agency (JST), Kawaguchi, Saitama 332-0012, Japan*
[4]*Synchrotron Light Application Center, Saga University, 1 Honjo, Saga 840-8502, Japan*

This study investigates the recombination dynamics in highly mismatched ZnTeO alloys using time-resolved photoluminescence (PL) spectroscopy. The large PL energy redshift with increasing O content and the disappearance of the ZnTe emission verify the O-induced conduction band anticrossing effect. The incorporation of O generates electron localization below the E_- conduction subband tail, which provide additional optical transitions and cause complex recombination mechanisms. Photoexcited free electrons in both the E_+ and the E_- conduction subbands favor rapid relaxation to low energy states. Additionally, temperature-independent long carrier lifetimes (>130.0 ns) that are induced by localized electrons increase with O concentration. © 2013 AIP Publishing LLC. [http://dx.doi.org/10.1063/1.4858968]

Dilute II-VI oxide semiconductors whose constituent anions are partially substituted by isovalent oxygen atoms of distinctly different electronegativity and size are commonly referred to as highly mismatched alloys (HMAs). ZnSeO and ZnTeO are the most widely studied examples of such HMAs, exhibiting multiple band gaps and giant band gap bowing.[1–8] The unusual energy band structures of these HMAs arise from the anticrossing interaction between the defect states of the substitutional minority O anions and the extended states of the host semiconductor matrix.[4,9] Since the electronegativity of the incorporated O atoms exceeds those of the host Se and Te atoms, isovalent defect states form near the conduction band edge (CBE). Accordingly, the interactions that occur in ZnSeO and ZnTeO are thought to be CB anticrossing (CBAC) such that the CB splits into two subbands (E_+ and E_-) with highly nonparabolic dispersion relations.[4,9] In ZnSeO, the O defect state is located within the CB of ZnSe, so a wide lower E_- band is formed through the anticrossing effect. However, a narrow lower band can be formed only if the defect state lies well below the CBE, and this situation occurs in ZnTeO.[4] Additionally, the strength of the anticrossing depends on the mismatch of electronegativities, which is more pronounced in ZnTeO than in ZnSeO because the mismatch between O and Te ($\Delta X = 1.4$) exceeds that between O and Se ($\Delta X = 1.1$). Therefore, in ZnTeO, the naturally formed narrow E_- band is highly separated from the higher-lying E_+ subband and acts as an intermediate band (IB), which provides additional optical transitions.

The IB concept was proposed as a solution to the efficiency problem because a partially filled narrow band that is isolated from the valance band (VB) and CB of a host semiconductor would allow the absorption of sub-bandgap energy photons. For photovoltaic solar cells, this process would result in the creation of additional electron-hole pairs and, in principle, an increase in the photocurrent without a decline in the open circuit voltage. Recently, Tanaka *et al.* demonstrated that the optical transitions that correspond to the E_+ and the E_- conduction subbands in ZnTeO ($0.04\% \le O \le 1.34\%$) films agree excellently with the BAC model and illustrate the proposed energy conversion mechanism for an intermediate band solar cell (IBSC).[7] They also presented strong experimental evidence for the generation of photocurrent by two-photon excitation in ZnTeO-based IBSC structures.[8] A solar cell with the IB as the stepping stone is essential for the realization of a highly efficient IBSC with a thermodynamic efficiency limit of 63.2%, which compares favorably with the Shockley-Queisser limit of 40.7% for a single band solar cell at optimal concentrations.[10,11] However, greater absorption of photons does not necessarily mean a larger photocurrent because rapid radiative and nonradiative recombination processes occur. Although much effort has been made to engineer the electronic band structures of ZnTeO, the details of the dynamics of carrier generation and recombination via the IB in this complex system remain unexplored. This study comprehensively investigates the emission and carrier decay dynamics in ZnTeO using temperature-dependent photoluminescence (PL) and time-resolved PL (TRPL) spectroscopy, which are of great importance for fundamental science and of particular relevance to the IBSC.

ZnTeO (O = 0.43, 0.77, and 1.09%) films were grown by radical source molecular beam epitaxy on ZnTe (001) substrates, following a procedure that has been published previously.[7] The thickness of all films was 0.6 μm. Their O content was determined by high-resolution X-ray diffraction (XRD) analysis, as described elsewhere.[7] PL and TRPL were excited using 200 ps pulsed laser diodes (377 or 638 nm/2.5 MHz/1 mW). A 377 nm continuous wave laser was used to make excitation power-dependent PL measurements. The PL and TRPL signals were dispersed using a Horiba iHR320 spectrometer with a 1200 g/mm grating and detected using an

---
a)Authors to whom correspondence should be addressed. Electronic addresses:
bryanlin@mail.nctu.edu.tw and wuchingchou@mail.nctu.edu.tw.

LN$_2$-cooled InGaAs photodiode and an Si photon-counting avalanche photodiode. The decay traces were recorded by time-correlated single photon counting (Time-Harp, PicoQuant).

Figure 1(a) shows the PL spectra of ZnTeO (O = 0.43, 0.77, and 1.09%) at 10 K. Notably, the spectra were obtained under an excitation energy of 3.29 eV (377 nm laser), which is well above the ZnTe band gap (~2.37 eV at 15 K)[12] and the ZnTeO E_+-VB transition (>2.40 eV at 10 K).[7] However, Fig. 1(a) presents only broad multi-peak emissions below 2.00 eV. Such broad emissions cannot be simply attributed to the direct E_--VB transition. Additionally, as the O content increases, the PL emissions shift rapidly downward in energy. The large PL energy redshift and the lack of ZnTe near-band-edge (NBE) emission upon the incorporation of O are strong evidence of the O-induced CBAC effect in ZnTeO. Accordingly, the absence of the E_+-VB transition in ZnTeO is attributable to the fast electron relaxation from the E_+ to the E_- or lower energy states and will be discussed later. Figure 1(b) shows the excitation power-dependent PL spectra of ZnTeO (O = 1.09%) at 10 K. The PL peaks are redshifted by ~100 meV and exhibited asymmetric bandwidth broadening as the laser power is reduced by two orders of magnitude. The huge PL peak energy redshift with decreasing power reveals that the density of states exhibits an exponential tail, which arises from O clustering or alloy fluctuations, indicating possible carrier localization. These results are highly consistent with the variance of O concentration in ZnTeO films that was determined by XRD and secondary ion mass spectroscopy because the O atoms are incorporated not only at substitutional sites but also at interstitial sites as O clusters.[7] Similar results were obtained from the other two samples over the same range of excitation power, revealing that the broad multi-peak emissions of ZnTeO are attributed to localized excitons. The electronic states that correspond to O provide a means to trap electrons from the E_+ and the E_- conduction subbands, and local regions of higher O concentration are associated with trapping states (traps hereafter) of lower energy and larger localization energies.

FIG. 2. (a) TRPL spectra of ZnTeO (O = 0.43, 0.77, and 1.09%) obtained at PL peaks under 377 nm excitation. Inset shows TRPL spectrum of ZnTeO (O = 1.09%) on a double logarithmic scale. (b) Schematic energy band diagram and associated optical transitions of ZnTeO. For simplicity, only one O trapping state is considered.

To gain insight into the recombination dynamics of ZnTeO, Fig. 2(a) shows the TRPL spectra at 10 K. Clearly, the PL lifetimes increase with the O content and are in the range of several tens to a few hundreds of nanoseconds. The PL decay traces exhibit nonsingle exponential decay and can be decomposed into an initial fast decline and a curved slow tail. The fast component exhibits mono-exponential decay, while the slow component cannot be traced by a single-exponential function. This behavior implies unusual (long decay lifetimes) and complex (curved slow profile) carrier decay dynamics in ZnTeO. To analyze the TRPL data, a four-level rate equation model, schematically depicted in Fig. 2(b), was first adopted. However, the standard analysis procedure fails to correlate well with the curved slow decay component, implying a wide and continuous distribution of O traps. Therefore, to obtain a more quantitative measure of the decay behavior, the decay curves are all fitted using the exponential equation, $I(t) = I_1 e^{-(t/\tau_1)} + I_2 e^{-(t/\tau_2)^\beta}$. The stretching exponent, $0 < \beta \leq 1$, is basically a measure of the relaxation rates that are involved in the PL decay process, where a smaller β represents a broader distribution of rates. Table I summarizes the decay coefficients that are derived from the fits to experimental data. Increasing the O concentration markedly increases τ_2 and reduces β. These phenomena are signatures of II-VI HMAs due to the increasing number of additional decay paths for electrons, implying that the slow decay originates in localized excitons.[3,13] Moreover, increasing the O content substantially reduces/increases the magnitude of the fast/slow decay component (I_1/I_2). These facts reveal that the entire PL decay profile
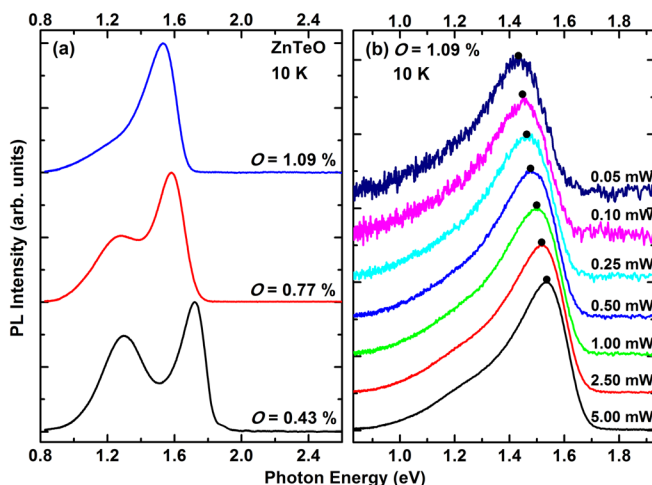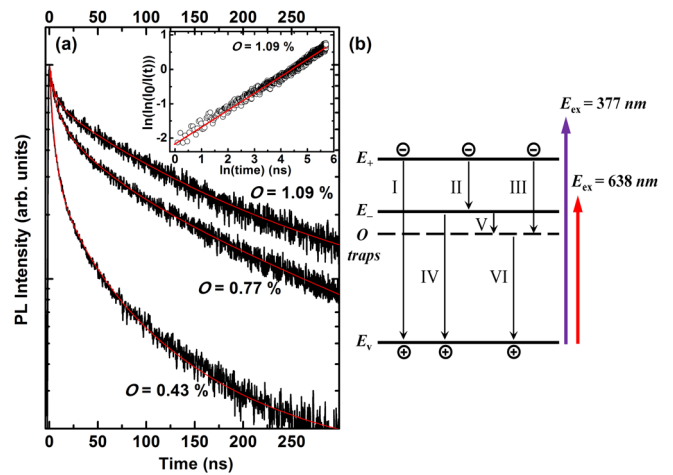

FIG. 1. (a) PL spectra of ZnTeO (O = 0.43, 0.77, and 1.09%) under 377 nm excitation. (b) Excitation power-dependent PL spectra of ZnTeO (O = 1.09%) with peak positions indicated.

TABLE I. Fitting parameters of TRPL spectra in Fig. 2(a). I_n and τ_n are amplitudes as percentages of the total signal and PL lifetimes, respectively, for n = 1 and 2.

O content (%)	I_1 (%)	τ_1 (ns)	I_2 (%)	τ_2 (ns)	β
0.43	60	3.6	40	29.0	0.70
0.77	20	6.0	80	106.5	0.62
1.09	5	6.3	95	134.8	0.52

gradually becomes a simple stretched exponential decay, $I(t) = I_0 e^{-(t/\tau)^\beta}$, in which the decay curve on a double logarithmic scale is a straight line, as is the case for ZnTeO (O = 1.09%), displayed in the inset in Fig. 2(a).

Figure 2(b) shows the energy band diagram and the associated optical transitions of ZnTeO. Under 377 nm excitation, the initial fast decay of ZnTeO can be ascribed to the following effects. (i) The radiative recombination of electrons directly from the E_- to the VB (channel IV). (ii) The radiative recombination of electrons directly from the high-energy O traps (electrons that do not hop toward low-energy traps) to the VB (channels VI). The nonradiative recombination is negligible since the PL is dominated by the radiative recombination at low temperature. The direct E_--VB transition could occur only in ZnTeO (O = 0.43%) because its PL emission at high energy shoulder is close to the transition edge. To verify this claim, Fig. 3(a) shows the TRPL spectra of ZnTeO (O = 0.43%) at various monitored energies. Obviously, the decay time from the slow component sharply falls as the monitored energy increases, while that from the fast component is insensitive to energy. The values of τ_1, τ_2, and β are 1.7/5.8 ns, 10.4/83.5 ns, and 0.72/0.52, respectively, at 1.83/1.28 eV. This behavior implies that the electrons transfer from shallow to deep O traps.[3,13] Moreover, monoexponential decay dominates the overall PL decay profile at high energy, becoming even more pronounced upon the recording of the high-energy emissions. The above results confirm the contribution of the E_--VB transition in ZnTeO (O = 0.43%), which is responsible for the huge initial rapid decay, as shown in Fig. 2(a). Hence, the recombination of electrons directly from the higher lying O traps to the VB is the main cause of the initial fast decay in ZnTeO (O = 0.77 and 1.09%).

The TRPL spectra of ZnTeO (O = 0.77%) at 10 K under 377 and 638 nm excitation, shown in Fig. 3(b), further confirm the aforementioned fast carrier decay. Clearly, the spectrum obtained under 638 nm excitation exhibits faster initial decay and a larger initial decay component than that obtained using the 377 nm laser. Restated, the initial fast decay is greatly suppressed under 377 nm excitation. Similar results were observed in ZnTeO (O = 0.43 and 1.09%).
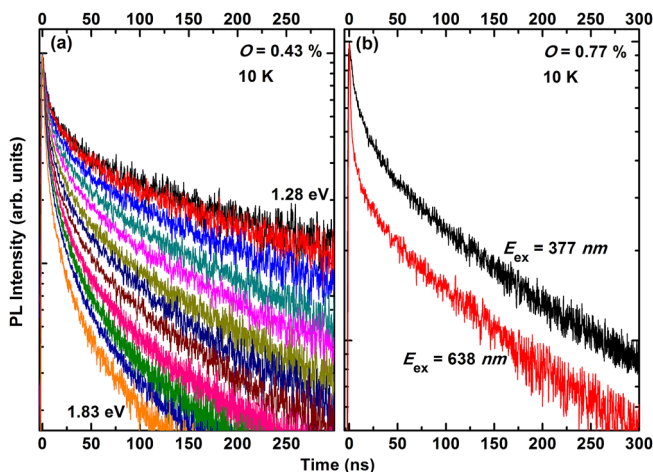
These phenomena are attributable to the feeding of photo-excited electrons from the E_+ to low-energy states [channels II and III in Fig. 2(b)], which increases the carrier delay times of channels IV and VI during the first few nanoseconds following excitation. These results further verify the rapid electron relaxation from the E_+ to the E_- or lower-energy states, which is responsible for the absence of the PL emission associated with direct E_+-VB transition [channel I in Fig. 2(b)].

To clarify further the dependence of the carrier dynamics in ZnTeO on temperature, Fig. 4(a) shows the temperature-dependent PL spectra of ZnTeO (O = 1.09%) with peak positions indicated. As the temperature increases, the PL peaks shift monotonically toward lower energies; these shifts are accompanied by asymmetric bandwidth broadening. The PL peaks are redshifted by ∼170 meV (10–120 K), which is larger than the shift of ZnTe NBE emission (∼120 meV; 15–300 K).[12] This feature is typical of carrier localization in a variable potential that is formed by the distribution of O traps. Above 70 K, the low-energy peak suddenly appears, which demonstrates that some of the trapped electrons gain extra energy to transfer into deeper O states. Figures 4(b) and 4(c) show the temperature-dependent TRPL spectra of ZnTeO (O = 1.09%) obtained under 377 and 638 nm excitation, respectively. Surprisingly, as revealed by Fig. 4(b), the decay curves are almost identical throughout the temperature range, except for their emission intensities. However, in Fig. 4(c), under 638 nm excitation, the initial fast decay, which is very strongly suppressed under 377 nm excitation, increasingly dominates the entire PL decay as the temperature increases. However, the slow decay remains almost unchanged. All of the studied ZnTeO films exhibit similar behavior. Notably, the excitation source is fixed at low power (∼1 mW) throughout this work, and spectra at higher temperatures can be obtained using high-power lasers. The huge PL decay upon increasing temperature can be readily understood as follows. In ZnTeO, the photoexcited electrons are localized in the nearest potential O traps, while holes are more weakly bound by a Coulomb force. As the temperature increases, the majority holes tend
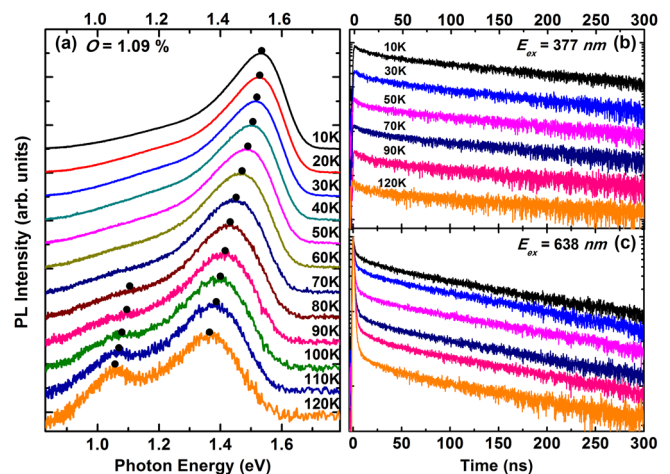

FIG. 3. TRPL spectra of (a) ZnTeO (O = 0.43%) for monitored energies from 1.83 to 1.28 eV under 377 nm excitation and (b) ZnTeO (O = 0.77%) monitored at PL peak under 377 and 638 nm excitation.

FIG. 4. (a) Temperature-dependent PL spectra of ZnTeO (O = 1.09%) under 377 nm excitation and corresponding TRPL spectra obtained at PL peaks under (b) 377 nm and (c) 638 nm excitation. Spectra in (b) at various temperatures are vertically shifted for clarity.

to reach an equilibrium distribution between the negative charged O traps and the VB. Thus, the weakly bound holes are away from the strongly localized electrons. Since the PL intensity falls, it is concluded that the thermally delocalized electrons recombine rapidly with the ionized holes nonradiatively. Restated, these experimental results indicate the emergence of thermally induced nonradiative recombination channels, which trigger the ultra-fast decay at high temperatures. This phenomenon is undoubtedly a major deficiency inherent in the material that is responsible for the still low conversion efficiency in ZnTeO-based IBSC to date.

In summary, this study investigated the time-resolved carrier dynamics in ZnTeO at various excitations energies and temperatures. The incorporation of O generates a wide distribution of electron localization below the energy of the E_- conduction subband, and these cause broad PL emission and serve as another IB. Decay curves that are induced by O traps exhibit nonsingle yet stretched exponential decay, and the corresponding temperature-independent long radiative lifetime ($\sim$135.0 ns for O $=$ 1.09%) increases with O concentration. However, electrons in both the E_+ and the E_- bands favor rapid relaxation to low energy states due to the intrinsic p-type behavior of ZnTeO and the emergence of O traps. Moreover, thermally induced rapid nonradiative recombination dominates carrier decay at high temperatures. These experimental results indicate that the recombination dynamics and carrier lifetimes of intermediate bands in ZnTeO can be engineered further by additional O and electron doping, which are now in progress.

[1]W. Shan, W. Walukiewicz, J. W. Ager III, K. M. Yu, J. Wu, E. E. Haller, Y. Nabetani, T. Mukawa, Y. Ito, and T. Matsumoto, Appl. Phys. Lett. **83**, 299 (2003).
[2]R. Broesler, E. E. Haller, W. Walukiewicz, T. Muranaka, T. Matsumoto, and Y. Nabetani, Appl. Phys. Lett. **95**, 151907 (2009).
[3]Y. C. Lin, H. L. Chung, W. C. Chou, W. K. Chen, W. H. Chang, C. Y. Chen, and J. I. Chyi, Appl. Phys. Lett. **97**, 041909 (2010).
[4]K. M. Yu, W. Walukiewicz, J. Wu, W. Shan, J. W. Beeman, M. A. Scarpulla, O. D. Dubon, and P. Becla, Phys. Rev. Lett. **91**, 246403 (2003).
[5]W. Wang, A. S. Lin, and J. D. Phillips, Appl. Phys. Lett. **95**, 011103 (2009).
[6]T. Tanaka, K. M. Yu, A. X. Levander, O. D. Dubon, L. A. Reichertz, N. Lopez, M. Nishio, and W. Walukiewicz, Jpn. J. Appl. Phys. **50**, 082304 (2011).
[7]T. Tanaka, S. Kusaba, T. Mochinaga, K. Saito, Q. Guo, M. Nishio, K. M. Yu, and W. Walukiewicz, Appl. Phys. Lett. **100**, 011905 (2012).
[8]T. Tanaka, M. Miyabara, Y. Nagao, K. Saito, Q. Guo, M. Nishio, K. M. Yu, and W. Walukiewicz, Appl. Phys. Lett. **102**, 052111 (2013).
[9]W. Shan, W. Walukiewicz, J. W. Ager III, E. E. Haller, J. F. Geisz, D. J. Friedman, J. M. Olson, and S. R. Kurtz, Phys. Rev. Lett. **82**, 1221 (1999).
[10]A. Luque and A. Martí, Phys. Rev. Lett. **78**, 5014 (1997).
[11]W. Shockley and H. J. Queisser, J. Appl. Phys. **32**, 510 (1961).
[12]Y. T. Shih, W. C. Chiang, C. S. Yang, M. C. Kuo, and W. C. Chou, J. Appl. Phys. **92**, 2446 (2002).
[13]Y. C. Lin, W. C. Chou, W. C. Fan, J. T. Ku, F. K. Ke, W. J. Wang, S. L. Yang, W. K. Chen, W. H. Chang, and C. H. Chia, Appl. Phys. Lett. **93**, 241909 (2008).